

# Double Stress Overshoot in Start-Up of Simple Shear Flow of Entangled Comb Polymers

F. Snijkers,<sup>\*,†</sup> D. Vlassopoulos,<sup>†,‡</sup> G. Ianniruberto,<sup>§</sup> G. Marrucci,<sup>§</sup> H. Lee,<sup>||</sup> J. Yang,<sup>||</sup> and T. Chang<sup>||</sup>

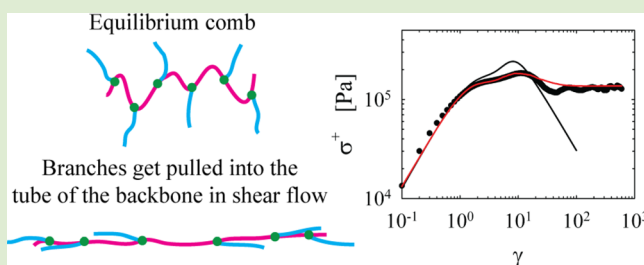
<sup>†</sup>Institute of Electronic Structure and Laser, FORTH, Heraklion 71110, Crete, Greece

<sup>‡</sup>Department of Materials Science & Technology, University of Crete, Heraklion 71003, Crete, Greece

<sup>§</sup>Department of Chemical Engineering, Materials and Industrial Production, University of Naples Federico II, P. le Tecchio 80, 80125 Naples, Italy

<sup>||</sup>Department of Chemistry and Division of Advanced Materials Science, Pohang University of Science and Technology (POSTECH), Pohang 790-784, Korea

**ABSTRACT:** We report on the unusual response of a well-characterized entangled comb polymer in simple shear flow. The polymer with highly entangled backbone (about 16 entanglements) and on average 29 long branches (about 3 entanglements each) has been extensively characterized by interaction chromatography and its rheology carefully studied under controlled conditions using a special cone partitioned-plate geometry. We observe that the start-up shear stress becomes roughly rate independent above a certain critical rate, related to the relaxation time of the branches. Within the rate-independent region, the start-up shear stress displays a double overshoot. We interpret these observations in light of tube-based pom-pom dynamics. The key idea is that for sufficiently long branches the main stress overshoot, which reflects backbone stretching and orientation, is preceded by the withdrawal of branches into the backbone tube. The excellent quantitative comparison between the simulations and experiments supports the proposed mechanism of the double stress overshoot.



Entanglement dynamics remains a challenging topic in polymer science.<sup>1</sup> The tube model originating from de Gennes<sup>2</sup> and Doi and Edwards<sup>3</sup> constitutes the basis for interpreting stress relaxation. The model was originally developed to describe the response of linear monodisperse polymers, but its current ramifications include accurate, nearly parameter-free predictions for the linear and nonlinear deformations of linear and architecturally complex polymers of varying polydispersity.<sup>1,4–7</sup> On the experimental side, advances in synthesis, characterization, and rheometry offer the possibility to obtain reliable information on the rheology of well-defined model polymers.<sup>8–14</sup> Despite these developments, in some respects the field is still at its infancy: in particular, linking molecular characteristics to the nonlinear rheological response, which is crucially important, has not been explored much yet; hence, the road toward a full understanding of the behavior of complex polymers in complex flows is still long.<sup>1,14</sup>

The start-up behavior of linear entangled polymers in simple shear has been studied quite extensively.<sup>5,8,9,15,16</sup> At rates below the inverse terminal relaxation time of the polymer  $1/\tau_0$ , the transient viscosity follows a monotonic increase toward the steady state, following the linear viscoelastic (LVE) behavior. At rates between  $1/\tau_0$  and the inverse Rouse time of the polymer ( $1/\tau_R$ ), the transient viscosity displays an overshoot before reaching a steady value, below the LVE one. This overshoot arises due to orientation of the chain in the flow direction, and the strain at the peak viscosity  $\gamma_{MAX}$  occurs at a constant value

of about 2.3. At rates above  $1/\tau_R$ , the overshoot becomes more prominent, while the steady viscosity is further reduced. The strain at the peak  $\gamma_{MAX}$  is no longer constant but proportional to the rate. Here, the combined action of stretch and orientation of the linear polymer governs the overshoot.<sup>5</sup> Tube models accounting for chain orientation alone do not predict a steady state for the viscosity at high shear rates. An additional mechanism, termed convective constraint release (CCR), has to be invoked to predict the steady-state and shear-thinning behavior of the viscosity in fast shear flows.<sup>17</sup>

There is only fragmental information in the literature on the shear flow of model branched polymers. The start-up and relaxation of stress of well-characterized comb polymers in simple shear was recently reported.<sup>10</sup> Such systems with several (about 30) but reasonably small branches (not exceeding two entanglements) and well-entangled backbones (about 16 entanglements) were found to respond like entangled linear polymers, when the dynamic dilution of the branches was accounted for. The overshoot of transient stress at large rates reflected backbone stretch and orientation. This main result was consistent with the behavior of the same and other branched polymers with more than one branch point (e.g., pom-pom) in uniaxial extension, as observed experimentally<sup>18,19</sup>

Received: May 11, 2013

Accepted: June 12, 2013

Published: June 14, 2013

and recently analyzed using tube-model arguments.<sup>20</sup> On the other hand, experimental start-up shear curves with highly branched commercial polymers (styrene-butadiene rubber, SBR) displayed multiple peaks,<sup>21</sup> which were found to relax and reappear only after long resting times and rationalized by invoking the pom-pom model and the idea of arm withdrawal.<sup>22</sup> In view of this, the fundamental question is whether a more complex response of entangled comb polymers emerges as their branches become larger and how this could be explained at the molecular level.

In this letter, we report on the start-up simple shear flow behavior of a well-defined, comb polymer with long branches. It is similar to those studied recently<sup>10</sup> but has longer branches (about three entanglements). This polystyrene comb (coded as PS c642)<sup>11–13</sup> was synthesized by Roovers using high-vacuum anionic polymerization.<sup>11</sup> It has a very narrow distribution with a backbone molar mass  $M_{\text{backbone}}$  of 275 kg/mol and an average of 29 branches randomly grafted on the backbone, each having a molar mass of 47 kg/mol. Its linear viscoelastic response has been studied in great detail and was found to be governed by hierarchical relaxation and dynamic dilution.<sup>12,13</sup> We performed an extensive physicochemical characterization using both the conventional size-exclusion chromatography (SEC) and temperature-gradient interaction chromatography (TGIC),<sup>23,24</sup> as well as linear oscillatory rheometry. TGIC is known to be extremely sensitive to side products produced during the synthesis of the comb polymer. The experimental details for the chromatography are identical to those in ref 10. The chromatograms are shown in Figure 1. The weight-averaged

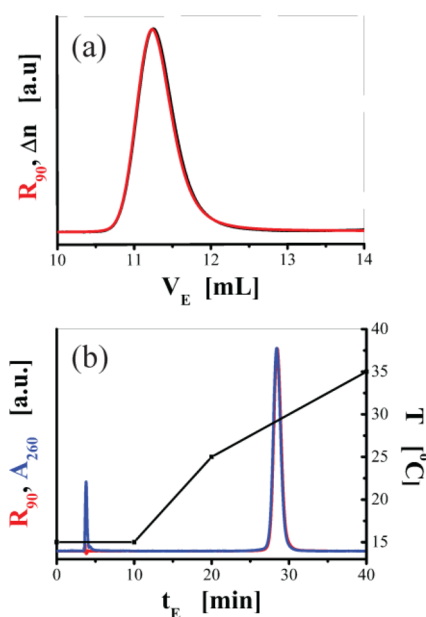


**Figure 1.** Chromatograms from SEC (a) and TGIC analysis (b).

molar mass  $M_w$  obtained from the SEC analysis is 1640 kg/mol, and the polydispersity index is 1.003 (as determined by light-scattering detection with band broadening correction), in agreement with refs 10 and 11, indicating that the sample is still intact, while its architectural dispersity is small so that we can safely consider the target molecular structure in our analysis.

At 169.5 °C, the comb has a zero-shear viscosity  $\eta_0$  of  $(5.8 \pm 0.2) \times 10^5$  Pa·s and a recoverable compliance  $J_S^0$  of  $(17.6 \pm 0.9) \times 10^{-5}$  Pa<sup>-1</sup>, leading to a longest relaxation time  $\tau_0 = \eta_0 J_S^0$

of  $102 \pm 6$  s. The relaxation time of the branches is about 0.5 s.<sup>13</sup> This comb is specific in the sense that the amount of branching is very high; in fact, the volume fraction of backbone in the molecule is only 16%, while the relaxation times of branches and backbone remain well-separated. The hierarchical relaxation principle<sup>4</sup> indicates that, after their relaxation, the branches act as effective solvent for the backbone (note that we consider full dynamic dilution, although in reality this is not entirely correct<sup>25</sup>). In this sense, the high amount of branching implies that the number of entanglements of the backbone after relaxation of the branches is very low, only 2.5 (assuming a dynamic dilution exponent of 1 and a molar mass between entanglements  $M_e$  of 17 kg/mol<sup>12,13</sup>). In the linear response, this manifests itself as an apparent Rouse-like relaxation region for the backbone (i.e.,  $G' \approx G'' \sim \omega^{0.5}$ ).<sup>12,13</sup>

The nonlinear shear flow of polymer melts is known to be prone to instabilities. To minimize those problems, we employed a homemade cone-partitioned plate (CPP)<sup>16</sup> inspired by the pioneering works of Meissner<sup>26</sup> and Schweizer.<sup>15</sup> The CPP delays pronounced effects of edge fracture on nonlinear measurements and also to some extent minimizes wall slip.<sup>15,27</sup> Our setup has been successfully employed recently to study entangled linear and comb polymers with shorter branches.<sup>10,16</sup>

Figure 2 shows the start-up shear viscosity  $\eta^+$  as a function of time  $t$  (Figure 2a) and the shear stress  $\sigma^+$  versus strain  $\gamma$  (Figure

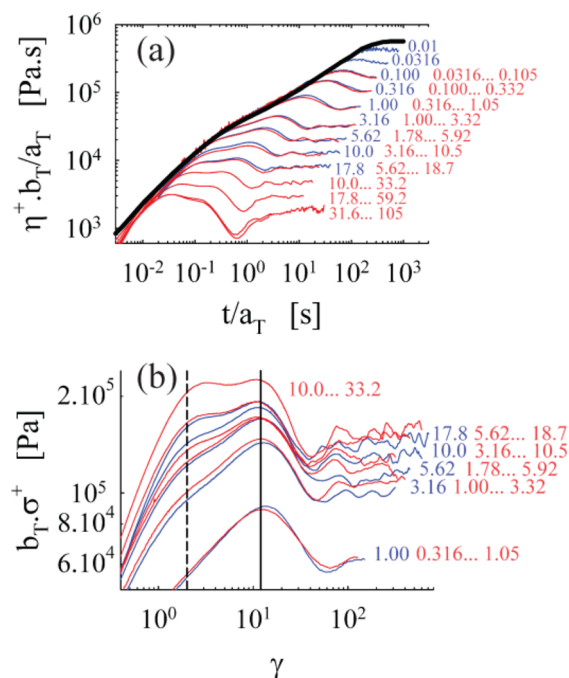


**Figure 2.** Start-up shear viscosity  $\eta^+$  versus time  $t$  (a) and stress  $\sigma^+$  versus strain  $\gamma$  (b) at 169.5 °C. The blue lines are obtained at 169.5 °C and the red lines at 160 °C and shifted. The shear rates are indicated (in s<sup>-1</sup>) next to the lines as “imposed rate... rate shifted to 169.5 °C”. The black line in (a) is the LVE line. The vertical straight lines in (b) are guides to the eye.

2b) for different rates. The blue lines are obtained at 169.5 °C and the red lines at 160 °C, and they are shifted using the time–temperature shift factors from the linear data.<sup>13</sup> The black line in Figure 2a is the LVE line obtained from the frequency sweep data<sup>12</sup> as in ref 10. The nonlinear data follows the LVE line for low rates and strains. Qualitatively, for rates

below  $\sim 2 \text{ s}^{-1}$ , one can observe a single peak, much like the situation for linear polymers<sup>8,9,16</sup> and combs with short branches.<sup>10</sup> At higher rates, an additional peak appears before the main one, which develops more clearly upon increasing rate. A plot of stress as a function of strain, as in Figure 2b, shows that both the stress and position of the peaks become roughly independent of rate (between  $\sim 3$  and  $30 \text{ s}^{-1}$ ). It is important to note in relation to the linear relaxation behavior that the rate of  $\sim 2 \text{ s}^{-1}$  is around the relaxation time of the branches.

Figure 3 shows the position of the two peaks  $\gamma_{\text{MAX}}$  as a function of shear rate. One can observe that initially the

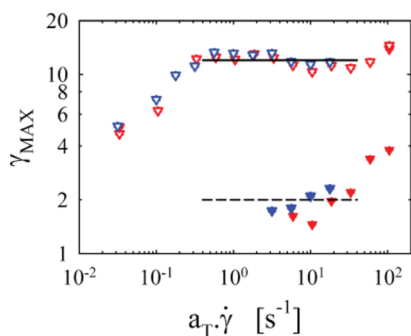


**Figure 3.** Strain at the peaks  $\gamma_{\text{MAX}}$  versus shear rate at  $169.5 \text{ }^\circ\text{C}$ . The blue symbols are obtained at  $169.5 \text{ }^\circ\text{C}$  and the red symbols at  $160 \text{ }^\circ\text{C}$  and shifted. The open and closed symbols correspond to the peak from the backbone and branches, respectively. Horizontal lines are guides to the eye.

(single) peak strain increases fast with rate, not necessarily with the same slope of linear polymers,<sup>16</sup> after which it levels off toward a constant value of 12–13, while an additional peak (from the branches) appears at a constant strain of about 2, the value for tube orientation. Finally, at the highest few rates both peaks can be observed to increase. The observed behavior for the peak strain (Figure 3) and the rate independence of start-up shear stress (Figure 2b) can be qualitatively explained by invoking the branch withdrawal idea, as done for SBR and schematically presented in Figure 4a.<sup>7,22</sup> We note that a double stress overshoot was reported for fast shear flows of bidisperse polymers when the stretch time of the larger component exceeded the terminal time of the shorter one.<sup>28</sup> The analogy with combs is the broad relaxation spectrum, but the phenomenology is different (the overshoots occurred at nearly constant time instead of strain, and a rate-independent region of the stress was never observed) and rationalized by weighting the stress contributions of the two components.<sup>29</sup>

To simulate the rate-independent behavior shown by the data in the neighborhood of  $10 \text{ s}^{-1}$  (Figures 2b and 3), we have developed the following statistical model. The model concentrates on the dynamics and stress contribution of the backbone only since the branches simply obey the Doi–Edwards orientation statistics, and their contribution to the stress can be added accordingly. Although the terminal relaxation time of the branches is (as previously mentioned<sup>13,25</sup>) large enough for the whole branches not to act as solvent, the end part of them is in fact free to fluctuate in the shear rate range considered. The solvent fraction affects the initial slope of the start-up curve (i.e., the initial level in a log–log plot), and we have therefore estimated that such a fraction is 0.3 (over a total branch fraction of 0.84). As a consequence,

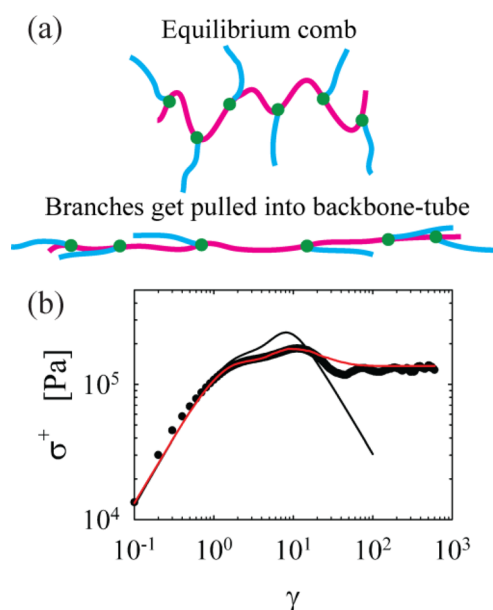


**Figure 4.** (a) Schematic representation of the branch withdrawal process. (b) Comparison between the data at a rate of  $10 \text{ s}^{-1}$  (black circles) and results of the simulations obtained with a dynamic dilution “solvent” fraction of 0.3. The red and black lines are for the simulations including CCR (with  $\beta = 0.5$ ) and without CCR, respectively.

for each molecule of the statistical ensemble, the initial conformation is a random walk of  $M_{\text{backbone}}/(M_e/0.7)$  steps (with a dynamic dilution exponent of 1), simulating the backbone tube at equilibrium. Backbone tubes then start deforming by small deformation increments, and all entanglements move affinely in space. The tube length increases with increasing deformation; i.e., the backbone gets stretched, and the tension in the backbone segments increases above the equilibrium value. Sufficiently large values of the tension determine arm withdrawal (Figure 4a).<sup>7,22</sup> The upper limit of tension is twice the equilibrium value for the two end segments of the backbone, three times the equilibrium value for the two next-to-end segments, four times for the next ones, and so forth up to 14 times the equilibrium tension for the middle segments of the 29-arm comb polymer. The shear stress contributed by the backbone then results from the combination of both stretch and orientation. The former monotonically increases up to saturation (when all branches are withdrawn), while the latter goes through the Doi–Edwards maximum at a strain of 2.3. The combined effect is a maximum occurring at a strain of about 10 (when non-Gaussian effects are accounted for), as shown in Figure 4b. The black curve in Figure 4b arises from the model as described above, to which the contribution of the orienting part of the branches has also been added (determining the shoulder in the stress at a strain of about 2.3). The red curve was obtained by including the effect of CCR. Indeed, without CCR the stress asymptotically approaches zero due to complete alignment to the shear direction in the basic Doi–Edwards theory. Inclusion of CCR requires one additional parameter, and we have here used the classical value<sup>17</sup>  $\beta = 0.5$  that nicely fits the asymptotic value shown by the data at  $10 \text{ s}^{-1}$ . CCR is implemented in the code both by including a  $\beta$ -dependent probability of losing entanglements (which somewhat relaxes the backbone stretch) and by explicitly correcting for the nonaffine orientation in the

stress. The simulated curve including CCR fits the data throughout, except for the undershoot shown by the data soon after the maximum.

One may further note that, while the location of the maximum remains fixed in the shear rate range considered, a weak rate dependence of the stress can be observed in Figure 2b, which is probably a signature of the rate dependence of the dynamic dilution of the outer parts of the branches (previously set to 0.3). To the left of the rate-independent region in Figure 3, the location of the maximum declines toward the purely orientational location (i.e., a strain of about 2.3), to eventually disappear altogether when the terminal relaxation is approached. To the right of the rate-independent region, i.e., for very large shear rates, a stretch of the arms appears to occur, determining a significant enhancement of the stress (Figure 2b). The shoulder contributed by the arms evolves toward a well-defined “first” maximum. Quantitative models for these regions have not yet been developed.

In conclusion, we have shown unambiguous evidence from experiments and simulations of the complex two-step stress evolution during start-up of simple shear flow of model comb polymers at high shear rates. It occurs only when the branches are sufficiently long, clearly more than two entanglement lengths, reasonably high in number (accounting for about 80% of the molar mass), and at rates exceeding the inverse of the relaxation time of the branches. Although our quantitative interpretation is sound, it involves some degree of speculation, and hence further work is needed to test it thoroughly. Nevertheless, these findings could provide a framework for understanding the complex nonlinear shear response of branched polymers. It would be interesting to test the observed phenomena as to their dependence on molecular parameters in a more systematic way and further make a link with the nonlinear response of commercial branched polymers and networks.<sup>21,30</sup>

## AUTHOR INFORMATION

### Corresponding Author

\*E-mail: frank@iesl.forth.gr

### Notes

The authors declare no competing financial interest.

## ACKNOWLEDGMENTS

Partial support from the EU (FP7 ITN DYNACOP grant 214627) and NRF (2008-0062045 and 2012R1A2A2A01015148) is gratefully acknowledged. We are grateful to J. Roovers for generously providing the polymer sample used in this work.

## REFERENCES

- (1) McLeish, T. C. B. *Adv. Phys.* **2002**, *51*, 1379.
- (2) de Gennes, P. G. *J. Chem. Phys.* **1971**, *55*, 572.
- (3) Doi, M.; Edwards, S. F. *J. Chem. Soc., Faraday Trans. 2* **1978**, *74*, 1789.
- (4) McLeish, T. C. B. *Europhys. Lett.* **1988**, *6*, 511.
- (5) Pearson, D.; Herbolzheimer, E.; Grizzuti, N.; Marrucci, G. *J. Polym. Sci., Part B* **1991**, *29*, 1589.
- (6) Graham, R. S.; Likhtman, A. E.; McLeish, T. C. B.; Milner, S. T. *J. Rheol.* **2003**, *47*, 1171.
- (7) McLeish, T. C. B.; Larson, R. G. *J. Rheol.* **1998**, *42*, 81.
- (8) Auhl, D.; Ramirez, J.; Likhtman, A. E.; Chambon, P.; Fernyhough, C. *J. Rheol.* **2008**, *52*, 801.
- (9) Menezes, E. V.; Graessley, W. W. *J. Polym. Sci., Polym. Phys. Ed.* **1982**, *20*, 1817.

- (10) Snijkers, F.; Vlassopoulos, D.; Lee, H.; Yang, J.; Chang, T.; Driva, P.; Hadjichristidis, N. *J. Rheol.* **2013**, in press.
- (11) Roovers, J. *Polymer* **1979**, *20*, 843.
- (12) Roovers, J.; Graessley, W. W. *Macromolecules* **1981**, *14*, 766.
- (13) Kapnistos, M.; Vlassopoulos, D.; Roovers, J.; Leal, L. G. *Macromolecules* **2005**, *38*, 7852.
- (14) McLeish, T. C. B.; Allgaier, J.; Bick, D. K.; Bishko, G.; Biswas, P.; Blackwell, R.; Blottiere, B.; Clarke, N.; Gibbs, B.; Groves, D. J.; Hakiki, A.; Heenan, R. K.; Johnson, J. M.; Kant, R.; Read, D. J.; Young, R. N. *Macromolecules* **1999**, *32*, 6734.
- (15) Schweizer, T.; van Meerveld, J.; Öttinger, H. C. *J. Rheol.* **2004**, *48*, 1345.
- (16) Snijkers, F.; Vlassopoulos, D. *J. Rheol.* **2011**, *55*, 1167.
- (17) Marrucci, G. *J. Non-Newtonian Fluid Mech.* **1996**, *62*, 279.
- (18) Nielsen, J. K.; Rasmussen, H. K.; Denberg, M.; Almdal, K.; Hassager, O. *Macromolecules* **2006**, *39*, 8844.
- (19) Lentzakis, H.; Vlassopoulos, D.; Read, D. J.; Lee, H.; Chang, T.; Driva, P.; Hadjichristidis, N. *J. Rheol.* **2013**, *57*, 605.
- (20) Ianniruberto, G.; Marrucci, G. *Macromolecules* **2013**, *46*, 267.
- (21) Bacchelli, F. *Kautsch. Gummi Kunstst.* **2008**, *April*, 188.
- (22) Marrucci, G.; Ianniruberto, G.; Bacchelli, F.; Coppola, S. *Prog. Theor. Phys. Suppl.* **2008**, *175*, 1.
- (23) Chang, T. *J. Polym. Sci. Polym. Phys. Ed.* **2005**, *43*, 1591.
- (24) Ryu, J.; Chang, T. *Anal. Chem.* **2005**, *77*, 6347.
- (25) Watanabe, H. *Prog. Theor. Phys., Suppl.* **2008**, *175*, 17.
- (26) Meissner, J.; Garbella, R. W.; Hostettler, J. *J. Rheol.* **1981**, *33*, 843.
- (27) Hatzikiriakos, S. G. *Polym. Eng. Sci.* **2000**, *40*, 2279.
- (28) Osaki, K.; Inoue, T.; Isomura, T. *J. Polym. Sci. Polym. Phys. Ed.* **2000**, *38*, 2043.
- (29) Islam, M. T. *Rheol. Acta* **2006**, *45*, 1003.
- (30) Boukany, P. E.; Wang, S. Q.; Wang, X. *Macromolecules* **2009**, *42*, 6261.